JOURNAL OF THE ROYAL SOCIETY Interface

Material properties of brachiopod shell ultrastructure by nanoindentation

Alberto Pérez-Huerta, Maggie Cusack, Wenzhong Zhu, Jennifer England and John Hughes

J. R. Soc. Interface 2007 **4**, 33-39
doi: 10.1098/rsif.2006.0150

JOURNAL OF THE ROYAL SOCIETY Interface

J. R. Soc. Interface (2007) **4**, 33–39
doi:10.1098/rsif.2006.0150
Published online 31 August 2006

Material properties of brachiopod shell ultrastructure by nanoindentation

Alberto Pérez-Huerta[1], Maggie Cusack[1,*], Wenzhong Zhu[2], Jennifer England[1] and John Hughes[2]

[1]*Department of Geographical and Earth Sciences, University of Glasgow, Glasgow G12 8QQ, UK*
[2]*Scottish Centre for Nanotechnology in Construction Materials, School of Engineering and Sciences, University of Paisley, Paisley PA1 2BE, UK*

Mineral-producing organisms exert exquisite control on all aspects of biomineral production. Among shell-bearing organisms, a wide range of mineral fabrics are developed reflecting diverse modes of life that require different material properties. Our knowledge of how biomineral structures relate to material properties is still limited because it requires the determination of these properties on a detailed scale. Nanoindentation, mostly applied in engineering and materials science, is used here to assess, at the microstructural level, material properties of two calcite brachiopods living in the same environment but with different modes of life and shell ultrastructure. Values of hardness (H) and the Young modulus of elasticity (E) are determined by nanoindentation. In brachiopod shells, calcite semi-nacre provides a harder and stiffer structure ($H \sim 3$–6 GPa; $E = 60$–110/120 GPa) than calcite fibres ($H = 0$–3 GPa; $E = 20$–60/80 GPa). Thus, brachiopods with calcite semi-nacre can cement to a substrate and remain immobile during their adult life cycle. This correlation between mode of life and material properties, as a consequence of ultrastructure, begins to explain why organisms produce a wide range of structures using the same chemical components, such as calcium carbonate.

Keywords: nanoindentation; brachiopod; biomineral; shell ultrastructure; ecology

1. INTRODUCTION

By the end of the Cambrian (*ca* 500 Ma), calcium carbonate biomineralization was predominant among invertebrate organisms secreting hard exoskeletons (Lowestam & Weiner 1989). This predominance of calcium carbonate (calcite and aragonite) was enhanced throughout the development of diverse biomineral fabrics with the subsequent radiation of numerous shell-bearing taxa at the beginning of the Ordovician. Within each phylum, a wide range of shell ultrastructures were developed reflecting diverse modes of life that require different material properties. Among marine sessile invertebrates, organisms that remain permanently cemented to a substrate during their adult life cycle (i.e. barnacles or craniid brachiopods) require more resilient structures to prevent breakage and damage than those organisms with higher degrees of mobility. However, our knowledge of how biomineral ultrastructure relates to material properties is still limited. The correlation between different biomineral structures and material properties is difficult to establish because it requires the determination of these properties on a detailed scale.

*Author for correspondence (maggie.cusack@ges.gla.ac.uk).

Electronic supplementary material is available at http://dx.doi.org/10.1098/rsif.2006.0150 or via http://www.journals.royalsoc.ac.uk.

Here, we use nanoindentation, mostly applied in engineering and materials science, to assess in detail the material properties of two calcite brachiopods living in the same environment but with different modes of life and shell ultrastructure. The craniid brachiopod, *Novocrania anomala*, has a shell of calcite semi-nacre and lives with the ventral valve cemented to a substrate. The rhynchonelliform brachiopod, *Terebratulina retusa*, is composed of calcite fibres and the shell is attached to a substrate via a pedicle, an arrangement that provides a higher degree of mobility. Therefore, calcite semi-nacre should provide a more robust calcite shell than that composed of calcite fibres. Values of hardness (H) and the Young modulus of elasticity (E) are determined by nanoindentation to test this hypothesis. In addition, a correlation between material properties and changes in shell ultrastructure is demonstrated.

2. BRACHIOPOD SHELL ULTRASTRUCTURE

Brachiopods are marine bivalved organisms that emerged in the Cambrian (*ca* 545 Ma) and are still cosmopolitan in distribution and habitat (Williams 1997*a*). They have been divided into three major subphyla based on shell mineralogy and ultrastructure (Williams *et al.* 1996). Two of these main groups, Craniiformea and Rhynchonelliformea, comprise taxa

Received 28 June 2006
Accepted 27 July 2006

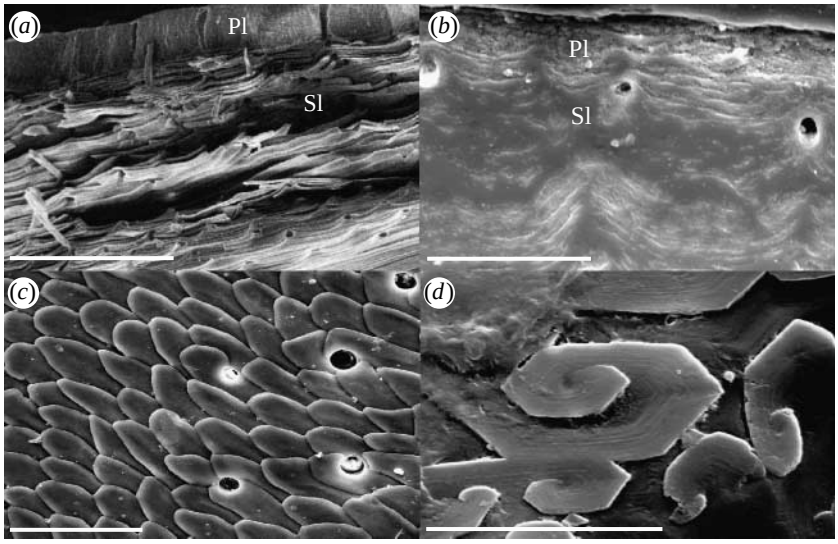

Figure 1. Scanning electron micrograph (SEM) of brachiopod shell ultrastructure: (*a*) *Terebratulina retusa* (scale bar, 200 µm) and (*b*) *Novocrania anomala* (scale bar, 100 µm; Pl, primary layer; Sl, secondary layer). Details of the shell ultrastructure in the secondary layer: (*c*) calcite fibres in *T. retusa* (scale bar, 50 µm) and (*d*) calcite semi-nacre in *N. anomala*, showing rhombohedral tablets with screw dislocation (scale bar, 5 µm).

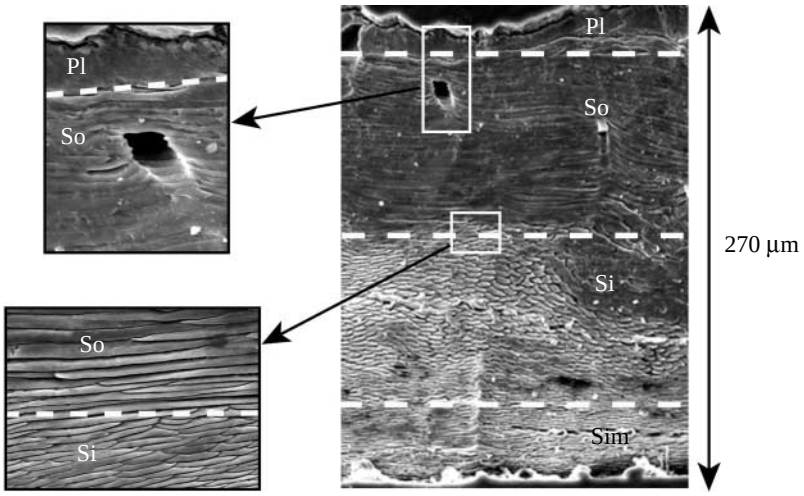

Figure 2. SEM showing in detail the shell ultrastructure of the anterior region of the dorsal valve of *Terebratulina retusa* and the interface between different layers (Pl, primary layer; So, outer secondary layer; Si, inner secondary layer; Sim, innermost secondary layer).

with calcite shells, but different ultrastructures reflecting dissimilar biomineralization processes. In Craniiformea, craniid brachiopod shells consist of an outer organic periostracum, a primary layer with acicular calcite and an innermost non-fibrous secondary layer of calcite semi-nacre (Williams & Wright 1970). The secondary layer is composed of laminae bearing rhombohedral tablets that grow spirally from single or double screw dislocations (Williams & Wright 1970; figure 1). Rhynchonelliform brachiopods also have a three-layered shell, but the secondary layer is composed of calcite fibres (Williams 1968; figure 1). This difference in shell fabrics of the secondary layer, which constitutes most of the shell, is regulated by the emplacement of proteins (Williams 1968; Williams & Wright 1970).

Details of the shell ultrastructure are presented in different regions of dorsal valves of a craniid brachiopod, *N. anomala*, and a rhynchonelliform brachiopod, *T. retusa*. *Novocrania anomala* displays a characteristic shell ultrastructure as previously described for craniiform brachiopods (Williams & Wright 1970). The thickness of the primary layer is about 20–30 µm and constant along the shell length. The thickness of the secondary layer varies, reaching up to 540 µm in the central region and not more than 400 µm in the anterior and posterior regions. *Novocrania anomal*a shells have a high concentration of organic material (Williams & Wright 1970; J. K. England 2005, unpublished Ph.D. thesis) and magnesium (Jope 1965; J. K. England 2005, unpublished Ph.D. thesis). In contrast, the shell ultrastructure of *T. retusa* is more complex than previously described for brachiopods of the order Terebratulida (Williams 1968). It is also composed of three layers, but there are differences in the thickness of the primary layer and the morphology and emplacement of calcite fibres within the secondary layer (figure 2). The thickness of the primary layer is variable (up to 50 µm) along the shell length, but it is very thin

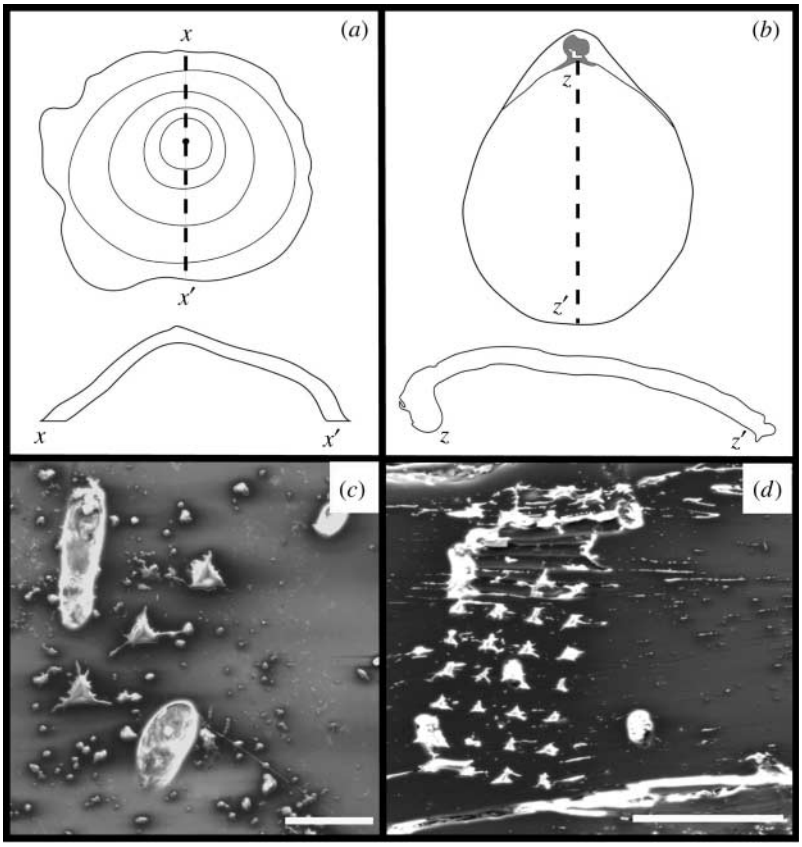

Figure 3. Schematic of (*a*) *Novocrania anomala* and (*b*) *Terebratulina retusa* and two-dimensional sections along the dorsal valve length from posterior to anterior regions (x–x' for *N. anomala* and z–z' for *T. retusa*). SEM showing: (*c*) three large indents in the central region of the dorsal valve of *N. anomala* (scale bar, 30 μm) and (*d*) small indents in the anterior region of the dorsal valve of *T. retusa* (scale bar, 100 μm).

in the posterior region (less than 20 μm) and absent in most of the umbonal region. The secondary layer can be further divided into three layers: outer (So); inner (Si) and innermost (Sim) (figure 2). The outer (So) layer is usually 100 μm thick and it is characterized by long and acicular fibres oriented parallel to the shell surface (longitudinally cut fibres; see Williams 1997*b*; Schmahl *et al.* 2004; Griesshaber *et al.* 2005*a*). However, the inner (Si) layer is similar in thickness with fibres that are oriented with the terminal faces normal to the plane of view (transverse sections of stacked fibres; see Williams 1997*b*; Schmahl *et al.* 2004; Griesshaber *et al.* 2005*a*; figure 2). The innermost part of the secondary layer (*ca* 30–50 μm in thickness) can be differentiated from the inner layer (Si), because the fibres have the same structural arrangement, but they are even more compactly set and there is an increase in organic content. This structural division of the secondary layer is apparent throughout the shell with the exception of the posterior region. In the posterior area, the shell is thinner (less than 200 μm) with the secondary layer composed only of long, acicular longitudinally cut fibres.

3. METHOD

3.1. Samples

Two recent species of calcite brachiopods, *T. retusa* and *N. anomala*, were used for this study. Articulated specimens of both brachiopods were collected at 200 m water depth from the same locality in the Firth of Lorne (Oban), northwest of Scotland. Two-dimensional sections of shell samples were obtained from posterior–anterior cuts along the plane of symmetry of the dorsal valves (figure 3). For comparison, only dorsal valves are used herein because ventral valves of craniid brachiopods, including those of *N. anomala*, are more weakly developed and differentially mineralized (Williams & Wright 1970; Cusack & Williams 2001).

Nanoindentations have to be performed in highly polished surfaces to avoid variations in results depending on the topographical effects (e.g. roughness). Two-dimensional sections of the dorsal valves were partially embedded in araldite resin, leaving the top surface free of any resin. Subsequently, the surface was ultra-polished initially with 6 and 3 μm thick diamond paste and finally polished using aluminium oxide (1 and 0.3 μm) and colloidal silica (0.6 μm) to avoid subsurface deformation. Nanoindentation experiments were conducted on these polished surfaces. Afterwards, sample surfaces were etched with 10% HCl acid and gold coated for scanning electron micrograph (SEM) observation (figures 2, 4 and 6), in an FEI 200F field-emission environmental scanning electron microscope, of the ultrastructure in areas where nanoindentations were performed.

3.2. Nanoindentation

Preliminary measurements of the material properties of biominerals (Lichtenegger *et al.* 2002), including brachiopods (Griesshaber *et al.* 2005*a*,*b*, 2006; Schmahl *et al.* 2006), have used nanoindentation. In this study,

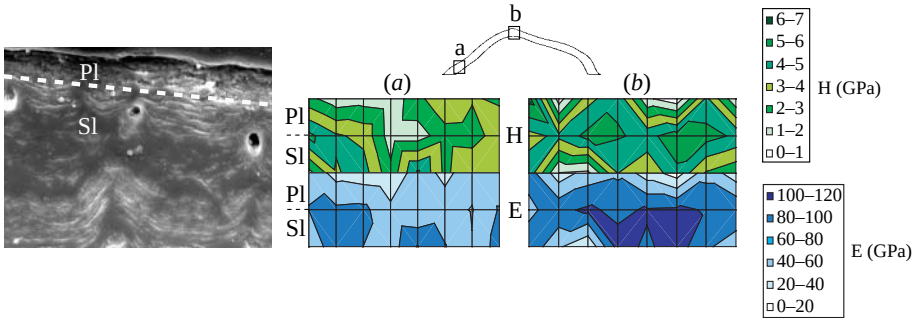

Figure 4. SEM of the transition between the primary (Pl) and the secondary (Sl) layers (figure 1). Maps of nanoindentation values of hardness (H) and elastic modulus (E) in the (a) posterior and (b) central regions of the dorsal valve of *Novocrania anomala* (area, 40 µm (vertical)×140 µm (horizontal; eight indents with 20 µm of separation)). (Enlargement of the figure and colour legends in the electronic supplementary material.)

nanoindentation measurements have been performed in three regions (posterior, central and anterior) along the dorsal valve length of *N. anomala* and *T. retusa*. Material properties have been assessed by establishing values of hardness (H) and the Young modulus of elasticity (E), which is referred to here as the elastic modulus. The nanoindentation apparatus used was Nanoindenter XP with a load range of 0–10 N (MTS Systems Corporation). The resolutions for load and displacement measurements are 50 nN and 0.04 nm, respectively. A diamond Berkovich tip was used for the test. Details of the technique have been presented and reviewed elsewhere (Oliver & Pharr 2004). In this study, all the testings were programmed in such a way that the loading started when the indenter came into contact with the test surface and the load maintained for 30 s at the pre-specified maximum value before unloading. The specimen's elastic modulus and hardness value are determined from the unloading curve of indentation test. Multiple loading–unloading cycles were applied at each test point, so as to allow assessment of the micromechanical properties at different length-scales to be made. Maximum loads of 50 and 5 mN were used for *T. retusa* and *N. anomala*, respectively, and the number of loads was between 3 and 5 cycles. Two to three large indents were made to provide points of reference (figure 3*c*) near the test area, where the indents were much smaller and sometimes difficult to find under microscope (figure 3*d*; see electronic supplementary material (ESM) for details of the individual test parameters).

4. RESULTS

4.1. *Novocrania anomala*

The assessment of material properties in *N. anomala* has been conducted at two different scales owing to the shell ultrastructure. Most of the shell thickness is composed of the secondary layer (Sl) with laminae of calcite semi-nacre (figure 1), while the primary layer (Pl) occupies only the outer 20–30 µm of the shell (figure 4). A detailed evaluation of hardness (H) and elastic modulus (E) using nanoindentation has been conducted at the interface between the primary and the secondary layers (figure 4) and across the secondary layer (figure 5).

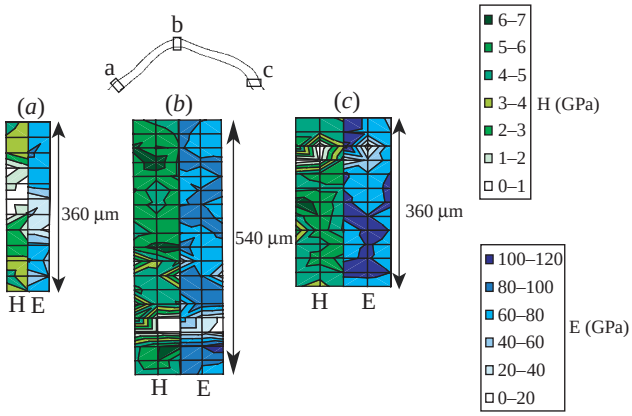

Figure 5. Maps of nanoindentation values of hardness (H) and elastic modulus (E) in the secondary layer of the (a) posterior (horizontal, 20 µm; two indents), (b) central (horizontal, 60 µm; three indents) and (c) anterior (horizontal, 60 µm; three indents) regions of the dorsal valve of *Novocrania anomala*. (Enlargement of the figure and colour legends in the electronic supplementary material.)

Measurements of the primary–secondary layer interface were conducted in the posterior (figure 4*a*) and central (figure 4*b*) regions along the dorsal valve length. The thickness of the primary layer is about 20 µm in both regions and nanoindentations were performed in an area of 40 µm (vertical)×140 µm (horizontal) (figure 4). In the posterior region (figure 4*a*), the primary layer is slightly softer (1–4 GPa) and less stiff (elastic modulus 20–60 GPa) than the secondary layer (H=2–5 GPa; E=40–80 GPa). In the central region (figure 4*b*), both the primary and secondary layers are more similar in terms of hardness and stiffness but within a wide range (H=1–6 GPa; E=20–120 GPa), although the secondary layer is relatively stiff. The overall comparison illustrates that the primary layer is slightly softer and more elastic in both regions.

A detailed study across the secondary layer has been conducted in three regions, with the same structure but differences in shell thickness, along the dorsal valve length (figure 5). For all regions, nanoindentations often came across punctae (perforations penetrating the shell; see Williams *et al.* 1997), with the resultant drop in the values of hardness (less than 2 GPa) and elastic modulus (less than 40 GPa).

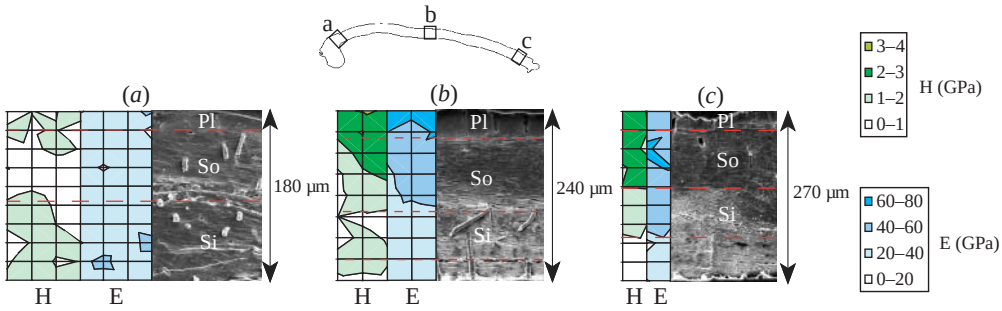

Figure 6. SEM of the shell ultrastructure and maps of nanoindentation values of hardness (H) and elastic modulus (E) in the (a) posterior (horizontal, 60 µm; four indents), (b) central (horizontal, 60 µm; three indents) and (c) anterior (horizontal, 30 µm; two indents) regions of the dorsal valve of *Terebatulina retusa*. (Enlargement of the figure and colour legends in the electronic supplementary material.)

The posterior (figure 5*a*) and anterior (figure 5*c*) regions are of equal thickness (360 µm), but the values of hardness and elastic modulus are quite different. The posterior regions are uniformly hard and stiff (H=2–4 GPa; E=60–80 GPa) across the thickness, except in a portion where nanoindentations came across a puncta. The anterior region also displays uniform hardness and stiffness, although the shell anterior is harder and stiffer than the posterior (H=4–5 GPa; E=80–100 GPa). However, the difference is that there are bands progressing across the central portion of the secondary layer thickness in the shell anterior, where values of hardness and stiffness increase (H>6 GPa and E>100 GPa; figure 5*c*). The central region (figure 5*b*) is thicker (540 µm) and has material properties similar to that of the anterior region (figure 5*c*). Hardness and stiffness are also uniform across the secondary layer in the central region of the shell (H=4–5 GPa; E=60–80 GPa). In contrast to the anteriord region, bands progressing across the secondary layer are thicker and more continuous, increasing the values of hardness up to 6–7 GPa and elastic modulus up to 100 GPa. Despite differences along the valve length, hardness and stiffness are fairly uniform in each region, although the central region is harder than the anterior and posterior regions, but it is as stiff as the anterior region. In addition, the anterior and central regions are harder and stiffer than the posterior region.

4.2. Terebratulina retusa

Values of hardness (H) and elastic modulus (E) have been determined by nanoindentation in three regions, with differences in shell ultrastructure, along the dorsal valve length (figure 6). The posterior region (figure 6*a*) is 180 µm thick and shows a uniform shell ultrastructure that can be divided into three layers: primary layer (Pl); outer secondary layer (So); and inner secondary layer (Si). The primary layer is thin (less than 20 µm) and the secondary layer is composed of long and acicular fibres, but fibres are more compact in the inner part than in the outer one. The overall values of hardness are low (0–2 GPa), but the primary and inner secondary layers are slightly harder than the outer secondary layer (figure 6*a*). The stiffness is uniformly low (20–40 GPa).

The central region (figure 6*b*) is 240 µm thick and also displays the same three characteristic layers. However, a thin portion of the innermost secondary layer can be distinguished based on the arrangement of calcite fibres, oriented with the terminal faces normal to the plane of view. In general, the hardness and stiffness decrease from the outside towards the inside of the shell. The primary layer (Pl) has values of hardness between 2 and 3 GPa and elastic modulus above 60 GPa. The outer secondary layer (So) has variable values of hardness (1–3 GPa) and elastic modulus (20–60 GPa), while the hardness and stiffness of the inner secondary layer (Si) is the lowest (H=0–2 GPa; E=20–40 GPa).

The anterior region (figure 6*c*) is similar to the central region in thickness (240 µm) and structure, but the characteristic highly compact set of fibres in the innermost part of the secondary layer is more developed. In contrast to the central region, the hardness of the primary and outer secondary layers is equal (2–3 GPa), while the stiffness (40–60 GPa) of the primary and inner secondary layers is constant. However, the inner secondary layer is less hard (0–2 GPa) and less stiff (20–40 GPa).

The combined analysis of material properties and shell ultrastructure determines that changes in values of hardness and stiffness correlate in general with structural differentiation. The primary and outer secondary layers are usually harder and stiffer than the inner part of the secondary layer. The morphology and arrangement of calcite fibres seems to determine the hardness and elastic properties within the secondary layer and, therefore, for most of the shell thickness. Thus, fibres that are oriented with the terminal faces normal to the plane of view (transversely cut) and more compact present lower values of hardness and stiffness. However, the degree of compaction of fibres seems to be more important than their orientation, as observed in the innermost part of the secondary layer (Sim; figure 6). Finally, the posterior region, which is less differentiated in terms of structure, is softer and more elastic than the central and anterior regions.

5. DISCUSSION

Nanoindentation was used to determine the values of hardness and elastic modulus with high spatial resolution along the dorsal valve of the shell of both

brachiopod species. The aim was to identify any correlation between material properties and shell ultrastructure that could improve our understanding of the suitability of specific ultrastructures for particular modes of life. In general, the results reveal such a correlation in both organisms. Prior to a comparison between brachiopod taxa, it is necessary to discuss general observations within the same species.

Novocrania anomala displays a relatively simple shell ultrastructure with a thin (20–30 μm) and uniform primary layer and a uniform secondary layer of calcite semi-nacre, which occupies most of the shell thickness. There are no significant differences in hardness and stiffness between the primary and the secondary layers despite the dissimilar calcite structure (i.e. Williams & Wright 1970). In general, values of hardness and elastic modulus in the secondary layer are quite uniform for each region of the valve (figure 5), but there are differences when comparing regions. The central region is harder and stiffer than the anterior and posterior regions. This is mainly explained owing to the presence of continuous and thick bands progressing from the outside to the inside, where values increase by an order of magnitude (figure 5*b*). There is no apparent explanation based on the structure, but it may reflect differences in crystallographic orientation of calcite crystals. Schmahl *et al.* (2004) suggested that different crystallographic orientations of calcite crystals provide distinctive material properties in some brachiopod shells. The change in crystallography also influences the material properties of nacre (e.g. Feng *et al.* 2000; Hou & Feng 2003). In addition, the posterior region is softer and more elastic than the central and anterior regions, possibly as a consequence of higher concentration of organics in this region. The values of hardness and elastic modulus ($H \sim 2$–5 GPa and $E \sim 60$–100 GPa) of *N. anomala* are close to or higher than those determined for inorganic calcite ($H > 3$ GPa and $E > 85$ GPa; e.g. Zügner *et al.* 2006). These data are in agreement with previous studies (Griesshaber *et al.* 2006), at least for *N. anomala*, where nanohardness and *E*-modulus of brachiopod calcite appear to be higher than those of inorganic calcite.

Terebratulina retusa is more complex and variable when observing the structure, but variations in material properties clearly correlate with structural differentiation (figure 6). An exception to this trend is observed in the posterior region, where values of hardness and elastic modulus are quite uniform across the valve thickness. The three typical structural layers, primary layer (Pl), outer (So) and inner (Si) secondary layers, can be recognized, but hardness and elastic modulus values are constant at 0–2 and 20–40 GPa, respectively (figure 6*a*). The constancy of hardness and stiffness may be explained because the primary layer is very thin and the secondary layer is only composed of loose and long calcite fibres oriented parallel to the shell surface. However, this posterior region is softer and less stiff when compared with other regions along the valve (figure 6), which may be explained by a higher concentration of organics. In contrast, the anterior and central regions reflect how the structure controls variations in material properties. The primary layer is hardest (2–3 GPa) and stiffest (greater than or equal to 60 GPa) despite being composed of acicular aggregates of calcite crystallites that deposit at fast rates (Williams 1968, 1997*b*). The outer part of the secondary layer (So) has material properties similar to that of the primary layer, with a minor drop in hardness and stiffness (figure 6), although it contains calcite fibres (figure 2). However, the inner part of the secondary layer (Si) is very distinct with lower values of hardness (0–2 GPa) and elastic modulus (20–40 GPa). This difference within the secondary layer is because the inner part is composed of fibres oriented with the terminal faces normal to the plane of view (figure 2). The innermost part of the secondary layer (Sim) has the same arrangement of fibres but highly compacted. The higher degree of compaction, which provides a better surface to distribute stress, is caused by a higher content of organic matrix bounding the fibres as observed under the SEM after acid etching. The organic content and compaction result in a softer and less stiff inner part of the secondary layer.

Detailed studies of material properties at this high spatial resolution provide bases for general comparison between brachiopod species. Although nanoindentation analyses were conducted in two-dimensional sections for the present study, it is possible to infer some general three-dimensional interpretations based on the studies of synthetic crystals (e.g. Schall *et al.* 2006). Thus, *N. anomala* is harder and stiffer ($H \sim 3$–6 GPa; $E = 60$–$110/120$ GPa) than *T. retusa* ($H = 0$–3 GPa; $E = 20$–$60/80$ GPa). These material properties are a consequence of the ultrastructure of the secondary layer, since it comprises the majority of the shell thickness. Therefore, calcite semi-nacre provides a harder and stiffer shell structure than calcite fibres. This would explain why craniid brachiopods, such as *N. anomala*, have advantage over rhynchonelliform brachiopods to securely attach their shells to any substrate. *Terebratulina retusa* attaches to a substrate using a pedicle, which gives them a certain degree of mobility, while *N. anomala* attaches to a substrate using its ventral valve and remains fixed and immobile during their adult life cycle. Having this fixed mode of life requires craniid brachiopods to develop harder and stiffer shells by using calcite semi-nacre to prevent breakage or damage by external factors (i.e. predatory action). This also begins to explain why organisms produce a wide range of structures using the same chemical components, such as calcium carbonate. In addition, the ability of organisms to produce minerals with different structures in acquiring certain material properties determines their capacity to adapt to different ecological niches in specific environments. Furthermore, this finding provides further understanding on the rapid diversification of shelly invertebrate faunas in benthic environments during the beginning of the Phanerozoic.

A.P.-H. (F0719AB) and J.E. (F/00179/X) thank the Leverhulme Trust for financial support. We would like to acknowledge thorough and helpful reviews by four anonymous referees and the editor, Dr T. Holt, which have considerably improved the quality of this manuscript. We also thank J. Gilleece, P. Chung, R. McDonald, L. Hill and Y. Finlayson for their technical support.

REFERENCES

Cusack, M. & Williams, A. 2001 Evolutionary and diagenetic changes in the chemico-structure of the shell of the cranioid brachiopods. *Palaeontology* **44**, 875–903. (doi:10.1111/1475-4983.00206)

Feng, Q. L., Cui, F. Z., Pu, G., Wang, R. Z. & Li, H. D. 2000 Crystal orientation, toughening mechanisms and a mimic of nacre. *Mater. Sci. Eng. C* **11**, 19–25. (doi:10.1016/S0928-4931(00)00138-7)

Griesshaber, E., Job, R., Pettke, T. & Schmahl, W. W. 2005*a* Micro-scale physical and chemical heterogeneities in biogenic materials: a combined micro-raman, chemical composition and microhardness investigation. In *Mechanical properties of bio-inspired and biological materials*, *MRS Symp. Proc. Series*, vol. 844 (ed. K. Katti, F. J. Ulm, C. Hellmich & C. Viney), pp. 93–98. Warrendale, PA: Materials Research Society.

Griesshaber, E., Schmahl, W. W., Neuser, R., Job, R., Bluem, M. & Brand, U. 2005*b* Microstructure of brachiopod shells: an inorganic/organic fibre composite with nanocrystalline protective layer. In *Mechanical properties of bio-inspired and biological materials*, *MRS Symp. Proc. Series*, vol. 844 (ed. K. Katti, F. J. Ulm, C. Hellmich & C. Viney), pp. 99–104. Warrendale, PA: Materials Research Society.

Griesshaber, E., Kelm, K., Sehrbrock, A., Job, R., Schmahl, W. W. & Mader, W. 2006 The ultrastructure of brachiopod shells: a mechanically optimized material with hierarchical architecture. In *Mechanical behavior of biological and biomimetic materials*, *MRS Symp. Proc. Series*, vol. 898E (ed. A. J. Bushby, V. L. Ferguson, C. C. Ko & M. L. Oye). Warrendale, PA: Materials Research Society.

Hou, W. T. & Feng, Q. L. 2003 Crystal orientation preference and formation mechanism of nacreous layer in mussel. *J. Cryst. Growth* **258**, 402–408. (doi:10.1016/S0022-0248(03)01551-3)

Jope, H. M. 1965 Composition of brachiopod shell. In *Treatise on invertebrate paleontology. Part H. Brachiopoda*, vol. 1 (ed. R. C. Moore), pp. 156–164. Boulder, CO; Lawrence, KS: The Geological Society of America; The University of Kansas Press.

Lichtenegger, H. C., Schöberl, T., Bartl, M. H., Waite, H. & Stucky, G. D. 2002 High abrasion resistance with sparse mineralization: copper biomineralization in worm jaws. *Science* **298**, 389–392. (doi:10.1126/science.1075433)

Lowestam, H. A. & Weiner, S. 1989 *On biomineralization*. New York, NY: Oxford University Press.

Oliver, W. C. & Pharr, G. M. 2004 Measurements of hardness and elastic modulus by instrumented indentation: advances in understanding and refinements to methodology. *J. Mater. Res.* **19**, 3–20. (doi:10.1557/jmr.2004.19.1.3)

Schall, P., Cohen, I., Weitz, D. A. & Spaepen, F. 2006 Visualizing dislocation nucleation by indenting colloidal crystals. *Nature* **440**, 319–323. (doi:10.1038/nature04557)

Schmahl, W. W., Griesshaber, E., Neuser, R. D., Lenze, A., Job, R. & Brand, U. 2004 The microstructure of the fibrous layer of terebratulide brachiopod shell calcite. *Eur. J. Miner.* **16**, 693–697. (doi:10.1127/0935-1221/2004/0016-0693)

Schmahl, W. W., Griesshaber, E., Neuser, R., Pettke, T. & Kelm, K. 2006 Texture and microstructure of terebratulid brachiopod shell calcite-A mechanically optimised material with hierarchical architecture. *In Micro- to nano-geosciences: developments and application*, p. 64. UK Mineralogical Society Winter Meeting, Programme and Abstract Volume.

Williams, A. 1968 *The evolution of the shell structure of articulate brachiopods In Special papers in palaeontology*, vol. 2. London, UK: The Palaeontological Association Press.

Williams, A. 1997*a* Preface. In *Treatise on invertebrate paleontology. Part H. Brachiopoda (Revised 1: introduction)*, (ed. R. L. Kaesler), pp. 1–6. Boulder, CO; Lawrence, KS: The Geological Society of America; The University of Kansas Press.

Williams, A. 1997*b* Shell structure. In *Treatise on invertebrate paleontology. Part H. Brachiopoda (Revised 1: introduction)*, (ed. R. L. Kaesler), pp. 267–320. Boulder, CO; Lawrence, KS: The Geological Society of America; The University of Kansas Press.

Williams, A. & Wright, A. D. 1970 *Shell structure of the Craniacea and other calcareous inarticulate Brachiopoda. In Special papers in palaeontology*, vol. 7. London, UK: The Palaeontological Association Press.

Williams, A., Carlson, S. J., Brunton, C. H. C., Holmer, L. E. & Popov, L. E. 1996 A supra-ordinal classification of the Brachiopoda. *Phil. Trans. R. Soc. B* **351**, 1171–1193.

Williams, A., Brunton, C. H. C. & MacKinnon, D. I. 1997 Morphology. In *Treatise on invertebrate paleontology. Part H. Brachiopoda (Revised 1: introduction)*, (ed. R. L. Kaesler), pp. 321–422. Boulder, CO; Lawrence, KS: The Geological Society of America; The University of Kansas Press.

Zügner, S., Marquardt, K. & Zimmermann, I. 2006 Influence of nanomechanical crystal properties on the comminution process of particulate solids in spiral jet mills. *Eur. J. Pharm. Biopharm.* **62**, 194–201. (doi:10.1016/j.ejpb.2005.08.002)